

Achieving a more realistic assessment of rockfall hazards by coupling three-dimensional process models and field-based tree-ring data

Daniel Trappmann,^{1*} Markus Stoffel^{1,2} and Christophe Corona^{1,3}

¹ Institute of Geological Sciences, University of Bern, Bern, Switzerland

² Climatic Change and Climate Impacts (C³i), Institute of Environmental Sciences, University of Geneva, Carouge-Geneva, Switzerland

³ Center National de Recherche Scientifique (CNRS) UMR6042 Geolab, Clermont-Ferrand Cedex, France

Received 3 October 2013; Revised 20 March 2014; Accepted 24 March 2014

*Correspondence to: Daniel Trappmann, Institute of Geological Sciences, University of Bern, Baltzerstrasse 1+3, CH-3012 Bern, Switzerland.
E-mail: daniel.trappmann@dendrolab.ch

ESPL

Earth Surface Processes and Landforms

ABSTRACT: Sound knowledge of the spatial and temporal patterns of rockfalls is fundamental for the management of this very common hazard in mountain environments. Process-based, three-dimensional simulation models are nowadays capable of reproducing the spatial distribution of rockfall occurrences with reasonable accuracy through the simulation of numerous individual trajectories on highly-resolved digital terrain models. At the same time, however, simulation models typically fail to quantify the ‘real’ frequency of rockfalls (in terms of return intervals). The analysis of impact scars on trees, in contrast, yields real rockfall frequencies, but trees may not be present at the location of interest and rare trajectories may not necessarily be captured due to the limited age of forest stands. In this article, we demonstrate that the coupling of modeling with tree-ring techniques may overcome the limitations inherent to both approaches. Based on the analysis of 64 cells (40 m × 40 m) of a rockfall slope located above a 1631-m long road section in the Swiss Alps, we illustrate results from 488 rockfalls detected in 1260 trees. We illustrate that tree impact data cannot only be used (i) to reconstruct the real frequency of rockfalls for individual cells, but that they also serve (ii) the calibration of the rockfall model Rockyfor3D, as well as (iii) the transformation of simulated trajectories into real frequencies. Calibrated simulation results are in good agreement with real rockfall frequencies and exhibit significant differences in rockfall activity between the cells (zones) along the road section. Real frequencies, expressed as rock passages per meter road section, also enable quantification and direct comparison of the hazard potential between the zones. The contribution provides an approach for hazard zoning procedures that complements traditional methods with a quantification of rockfall frequencies in terms of return intervals through a systematic inclusion of impact records in trees. Copyright © 2014 John Wiley & Sons, Ltd.

KEYWORDS: tree ring; dendrogeomorphology; 3D rockfall simulation models; rockfall frequency; hazard assessment

Introduction

Rockfall is a common but dangerous natural process in mountain environments and therefore needs a sound management to keep risks in endangered areas at an acceptable level. A rockfall is defined as a fragment of rock detaching from a release area to proceed downslope by bouncing, falling, or rolling (Varnes, 1978). Volumes of rockfalls are usually below 5m³ (Berger *et al.*, 2002). When rockfall prone areas intersect with human settlements or transportation lines, a detailed knowledge on rockfall hazards is required to provide a basis for alleviating the damaging effects of rockfalls to humans, their belongings and constructions (Crosta and Agliardi, 2003; Lateltin *et al.*, 2005). A key element in rockfall management is therefore the assessment and mapping of spatial and temporal probability of rockfall occurrences at the site under investigation (Abbruzzese *et al.*, 2009; Volkwein *et al.*, 2011).

Depending on their intensity and frequency, rockfall hazards are typically classified in varying degrees of danger, and defined as high, moderate or low hazard (Raetzo *et al.*, 2002). A commonly accepted criterion for intensity is the impact energy of falling rocks. Energies at any position along the fall path can be obtained through simulation runs with physically-based models that simulate rockfall trajectories on a slope surface and representative design blocks (Jaboyedoff *et al.*, 2005; Stoffel *et al.*, 2006; Dorren *et al.*, 2011). A verification of model results is crucial (Agliardi and Crosta, 2003; Berger and Dorren, 2006) and can commonly be achieved through field visits, the analysis of remotely sensed information (e.g. orthophotos) or archival records (Dorren and Berger, 2006).

By contrast, the assessment of frequencies has been proven more difficult in the past. At larger scales, rockfall frequency can be evaluated with statistical analyses of documented past rockfalls and the establishment of magnitude-frequency

relationships (e.g. Dussauge-Peisser *et al.*, 2002). For more detailed studies and at the slope scale, however, inventory data will remain unavailable, scarce or unreliable in most cases, and will thus prevent the application of statistical approaches. This is even more so the case in remote areas and for low-magnitude events with no damage (Guzzetti *et al.*, 2004; Corominas *et al.*, 2005; Stoffel *et al.*, 2006). Another possibility to derive onset frequencies is the long-term visual observation of cliffs (e.g. Matsuoka, 2008), but such data is only rarely available and can only cover small sites and comparably shorter time periods. Besides field accessibility, the temporal effort will be a limiting factor for any type of direct observation. As a consequence, the assessment of onset susceptibility has become a widely used alternative, as data can be obtained through a heuristic ranking of instability indicators or by deterministic or statistical methods (see Volkwein *et al.*, 2011, for a recent review). These approaches, in combination with the modeling of rockfall propagation, can yield valuable maps of rockfall susceptibility at the slope scale (Michoud *et al.*, 2012). However, for the purpose of rockfall management, reliable quantitative data will still be needed on rockfall frequencies, as it is a prerequisite for (i) the translation of susceptibility to hazard, (ii) any risk assessment, (iii) cost-benefit analyses of potential mitigation measures and fact-based prioritization of funding decisions.

Dendrogeomorphic techniques have been applied repeatedly to study the impact of rockfalls on trees. The coupling of rockfall impact number with tree age has been demonstrated repeatedly to be a reliable quantitative, indirect indicator of 'real' rockfall frequency and the spatial occurrence of past events (Corona *et al.*, 2013; Trappmann and Stoffel, 2013; Trappmann *et al.*, 2013). The term 'real rockfall frequency' is used here to characterize rockfall occurrences per time unit in contrast to 'simulated trajectories' or 'simulated passages' which characterize the spatial occurrence of rockfalls predicted by a rockfall simulation model. Early dendrogeomorphic research focused primarily on the analysis of impacts in conifer trees; the potential of broadleaves has been explored only in more recent studies (Arbellay *et al.*, 2010, 2012a, 2012b, 2013; Ballesteros *et al.*, 2010; Moya *et al.*, 2010b; Šilhán *et al.*, 2011, 2012). In contrast to conifers, broadleaved trees are often characterized by relatively thin and smooth bark structures which not only facilitate wounding but also enhance the visibility of completely overgrown scars. Many broadleaved species are thus suitable for the application of a scar count method where the number of past impacts is obtained through the counting of scars visible on the stem surface (Trappmann and Stoffel, 2013). This procedure has been demonstrated to be comparably suitable – yet slightly less precise – than classical tree-ring approaches, and to clearly allow a realistic quantification of rockfall activity in space and time with limited efforts and at reasonable cost (Trappmann and Stoffel, 2013; Trappmann *et al.*, 2013).

With the aim of improving rockfall hazard studies for environmental management purposes and in an attempt to further optimize analyses, this paper proposes a methodology for the assessment of rockfall frequencies by coupling field-based impact data from trees with three-dimensional (3D), process-based rockfall modeling approaches. We systematically analyzed a large number of trees within predefined raster cells on a rockfall slope above a road to (i) reconstruct the real frequency of rockfalls which affected the study area in the past, (ii) calibrate the rockfall model Rockyfor3D, and to (iii) use simulated trajectories to extrapolate real rockfall frequencies at the level of the road.

Study Site

The study site under investigation is located above a 1631-m long road section (central point 46° 8' 10''N, 7° 28' 20''E) of the cantonal road connecting Sion and Arolla (Evolène, Swiss Alps); it covers a surface of 8.8 ha with a mean slope gradient of 31° (see analysis cells in Figure 1 for details). The southwest-facing study reach belongs to the Siviez-Mischabel nappe and is comprised of gneisses, schists and amphibolites. Heterogeneously fractured bedrock forms widespread release areas of rockfall (Figure 1) that range from smaller outcrops in the forest with only a few m³ to large rock faces with several hundred m³ of material for potential rockfalls. Rockfall fragments vary from clasts with edge lengths of only a few decimeters to blocks with volumes > 10 m³. Scree slopes scattered over the slope, numerous traces of rockfall on the ground and several recent rockfall deposits that can be found below the cantonal road or in its direct proximity testify to frequent and contemporary rockfall activity at the site.

The slope is covered with a mixed forest stand with trees of different ages (Figures 2b and d) consisting predominantly of Silver birch (*Betula pendula* Roth), European larch (*Larix decidua* Mill.), Norway spruce (*Picea abies* (L.) Karst.) and European aspen (*Populus tremula* L.), and with frequent meadow patches in its lower part. In addition to the main road, a forestry road, electricity lines and hiking trails cross the slope and are exposed to rockfall hazards as well.

Archival records report on a limited number of recent rockfall events at the study site (Figure 2a). In 2005, for instance, a block of several m³ reached the road and in 2006, an estimated volume of 30 m³ was released and blocks of several m³ crossed or stopped at the road (BEG, Bureau d'Etudes Géologiques SA, 2006). Rockfall is the dominant geomorphic process operating at the site. No other geomorphic processes relevant for tree damage (such as e.g. snow avalanches or debris flows) occur at the site and thus damage in trees can be doubtlessly attributed to rockfall activity (Figure 2c).

Methods

Figure 3 describes the conceptual approach used in this paper to assess rockfall frequencies. The main steps of this procedure included (i) the analysis of rockfall scars and related dendrogeomorphic sampling (Stoffel *et al.*, 2010) to yield real rockfall frequencies; (ii) the calibration of the rockfall simulation

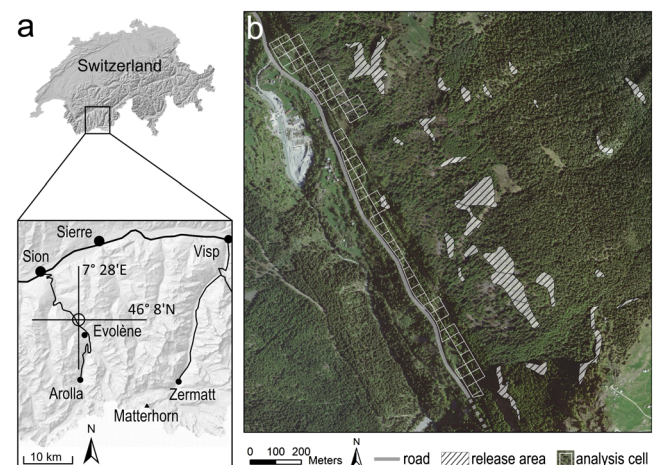


Figure 1. Overview on the study site. (a) Geographical location. (b) Aerial photograph of the studied road section with location of analysis cells above the road. This figure is available in colour online at wileyonlinelibrary.com/journal/esp

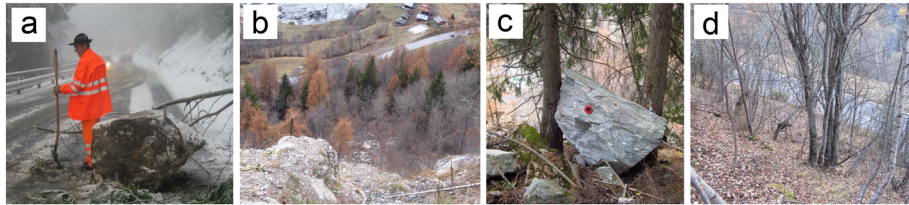


Figure 2. (a) Rockfall at the level of the road (source: BEG, Bureau d'Etudes Géologiques SA, 2006). (b) View on the study site from one of the major release areas. Note the forest composed of mature trees that are suitable for dendrogeomorphic analysis close to the level of the road. (c) Imprints of rockfall in the forest. (d) Area close to the road with young vegetation that is less suitable for dendrogeomorphic analysis. This figure is available in colour online at wileyonlinelibrary.com/journal/esp

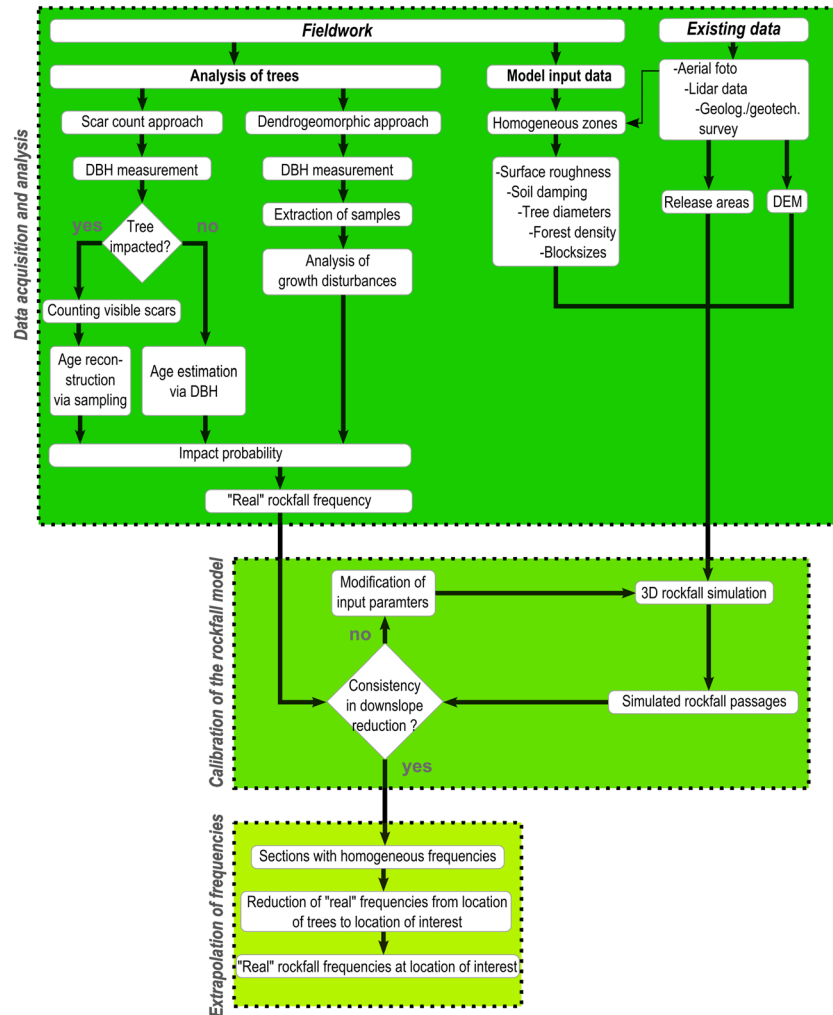


Figure 3. Conceptual model for rockfall hazard assessment combining tree-ring data and 3D rockfall simulation models. This figure is available in colour online at wileyonlinelibrary.com/journal/esp

model Rockyfor3D (Dorren, 2012) based on real frequencies; and (iii) the extrapolation of real frequencies at the level of the main road using the simulated rockfall trajectories.

Estimation of rockfall frequencies using tree injuries

Scar sampling was implemented in a way to acquire data for a very long road section but with reasonable temporal efforts. We first of all defined a grid with 40 m × 40 m cells and selected those cells located closest to the road and containing trees suitable for analysis. As a rule of thumb a minimum of 15 trees with a diameter at breast height (DBH) ≥ 10 cm were needed for a cell to be included for analysis. Where these requirements were not fulfilled, the cell was excluded. In case of insufficient tree number, additional cells were added further upslope. We

also excluded anthropogenic disturbances such as logging or construction activities so as to avoid misinterpretation and faulty attribution of injuries to rockfall activity. The 64 raster cells kept for analysis are oriented in a stretched raster in NW-SE direction and within 41 columns. In these cells, all trees ≥ 10 cm DBH were then investigated and their DBH measured, resulting in a dataset of 1260 trees.

On young conifers and broadleaved trees with a smooth bark structure, injuries remain visible on the stem surface for a long time. The number of impacts was therefore assessed visually in these trees by counting open and overgrown scars on the stem surface, provided that the scars had a meaningful geometry and location on the stem (i.e. excluding scars with unusual long vertical extent that might be caused by falling neighboring trees or bark stripping animals; excluding scars on the downslope side of the trunk). During fieldwork, we also observed multiple

scars on the same tree presumably inflicted by a single rock (similar appearance and close neighborhood of scars) and therefore counted these scars only once. If several scars could be detected that were rather distant, had different appearance or were located on different sides on the trunk, they were attributed to several rock impacts. Tree age was determined with increment cores taken from the downslope side of impacted trees and as close to the ground as possible. Cross-sections were taken only in a few exceptional cases from previously broken trunks using a handsaw.

Bark peeling is frequent in mature *Larix decidua* and *Picea abies* and will thus blur evidence of older rockfall on the stem surface and render a visual detection of scars almost impossible. As rockfall impacts will also leave typical growth disturbances in the tree-ring series, they can be used to detect past activity in the absence of visible signs on the stem surface. In the case of older trees, we therefore extracted several cores with increment borers (maximum 40 cm × 0.5 cm) from the upslope facing side of the trunk. In a few exceptional cases, wedges were taken with a handsaw to obtain a sample of the contact between the scar edge and intact wood tissues. The 'classic' dendrogeomorphic sampling was applied only to older conifers and with the idea to determine absolute numbers of impacts and to obtain their age.

All samples were processed with standard dendrochronological techniques (Bräker, 2002; Stoffel and Bollschweiler, 2008) which included sanding, tree-ring counting, as well as the analysis of growth disturbances such as tangential rows of traumatic resin ducts, callus tissue, or compression wood. In case that the pith

was not reached, we added missing rings towards the center using a transparent template of concentric rings (Bosch and Gutiérrez, 1999) and assuming growth rates similar to those observed on the five oldest rings present on the core (Rozas, 2003). We collected a total of 202 tree-ring samples within this study, composed of 195 increment cores, two cross-sections and five injury wedges.

The growth data gathered from the tree-ring samples was then used to derive a linear diameter-age regression model for each of the tree species investigated. This data was then used to estimate ages for uninjured trees and for trees where scars were counted on the stem surface and the DBH has been measured, but where, at the same time, no cores have been taken. Table I provides an overview of all species and the number of trees available in the 64 cells as well as on the number of samples taken per species.

We then computed rockfall frequencies for each analysis cell and included an estimation of rockfalls leaving no visible signs in the vegetation using the impact probability approach of Moya *et al.* (2010a). The 'conditional impact probability' (CIP) concept is based on the idea that each tree is surrounded by a 'circle of impact', i.e. that it covers a range of the slope which determines its probability of being impacted. A falling rock, however, will impact the tree if its trajectory is closer to the stem than half of its diameter. This 'circle of impact' can be expressed as a circular area around each tree with a diameter defined by the tree's DBH and the rock diameter. The sum of the impact circles of all trees from one cell represents the total length of impact circles (L_{ic}), or the range that is covered by trees in other words (Figure 4a). In line with this concept, we ignored trees that were located in the direct fall line of other trees and that would thus protect each other.

With a given mean rock diameter and measured DBH of all trees, the CIP can be calculated for each analysis cell as

$$CIP = \frac{L_{ic}}{L_{plot}} \quad (1)$$

where L_{ic} is the cumulated diameter of all impact circles and L_{plot} is the length of the plot (i.e. width of analysis cell; 40 m in this case).

At the study site, recent rockfall deposits with non-weathered surfaces and absence of moss or lichen cover have been measured to identify characteristic block sizes involved in rockfall activity and for each of the cells. Analysis was based on 176 recent rocks and allowed distinction of five zones with distinct homogeneous and distinct block diameters. Volumes of individual rockfall deposits are given per column in Figure 5.

Table I. Overview on investigated tree species and samples collected.

| Species | Number of trees | Percentage | Number of samples | Percentage |
|---------------------------------|-----------------|------------|-------------------|------------|
| <i>Betula pendula</i> Roth | 427 | 34 | 53 | 26 |
| <i>Larix decidua</i> Mill. | 213 | 17 | 56 | 28 |
| <i>Populus tremula</i> L. | 211 | 17 | 20 | 10 |
| <i>Picea abies</i> (L.) Karst. | 205 | 16 | 38 | 19 |
| <i>Fraxinus excelsior</i> L. | 54 | 4 | 7 | 3 |
| <i>Salix caprea</i> L. | 44 | 3 | 8 | 4 |
| <i>Acer pseudoplatanus</i> L. | 33 | 3 | 5 | 2 |
| <i>Alnus incana</i> (L.) Moench | 32 | 3 | 4 | 2 |
| <i>Sorbus aucuparia</i> L. | 24 | 2 | 5 | 2 |
| <i>Corylus avellana</i> L. | 10 | 1 | 3 | 1 |
| <i>Sorbus aria</i> (L.) Crantz | 4 | <1 | 2 | 1 |
| <i>Prunus avium</i> L. | 3 | <1 | 1 | <1 |
| Sum | 1260 | 100 | 202 | 100 |

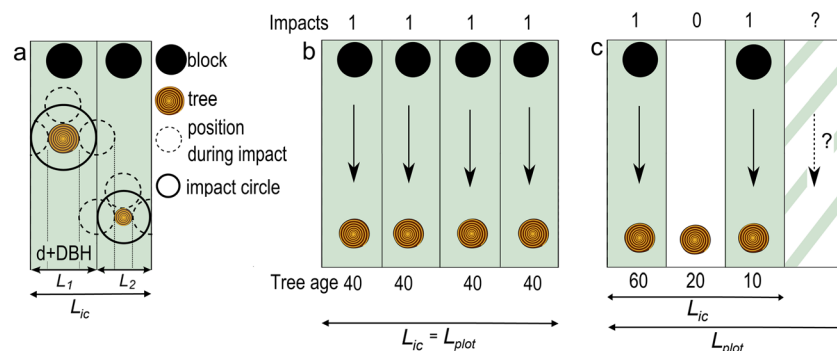


Figure 4. (a) The range covered by individual trees (projected impact circles L_1 , L_2) is defined by tree diameter (DBH) and block diameter (d) (after Moya *et al.*, 2010a). (b) Analysis cells with the complete cell width (L_{plot}) covered by trees will record all impacts. (c) Cells with only a portion of the cell width covered might not record all rockfall events and frequencies must be corrected considering impact probability. This figure is available in colour online at wileyonlinelibrary.com/journal/espl

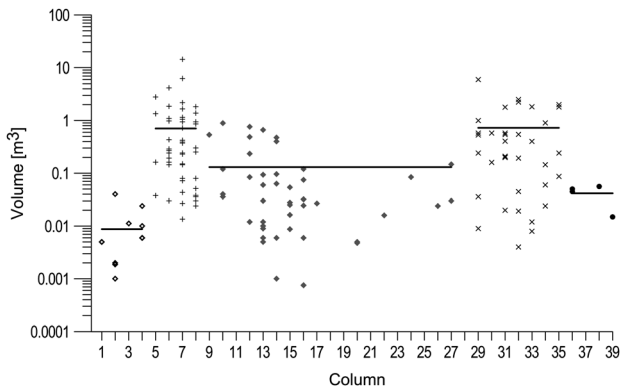


Figure 5. Volumes of recent rockfall deposits per column of the analysis raster (for location of columns, see Figure 9); volumes deposited in groups of columns with homogeneous block sizes are depicted with the same symbol; mean rock volumes as used for simulations and CIP calculation depicted as horizontal lines.

The particular mean block diameters for each column were then used to calculate the CIP for the corresponding cells.

The reconstruction of rockfall frequencies is illustrated in Figures 4b and c. In the simplified case given in Figure 4b, each range that is covered by trees is affected by exactly one rockfall during the lifetime of each tree. In this exemplary case, we assume that four rocks entered the cell over the course of 40 yr (i. e. mean age of trees in this example). The frequency of rocks entering the cell is four divided by 40, meaning 0.1 rocks yr^{-1} . In the more realistic case presented in Figure 4c, only two out of three trees were impacted by a rock in their lifetime (mean 30 yr) and only three out of four cells contain trees. In this case a CIP of 0.75 is applied which will yield two impacts

divided by $\text{CIP} = 0.75$, meaning 2.7 rocks entering the cell. The frequency F for this cell consequently is 2.7 rocks divided by 30 yr, resulting in $0.09 \text{ rocks yr}^{-1}$, using Equation 2:

$$F = \frac{I_{\text{total}}}{(a_{\text{mean}} \times \text{CIP})} \quad (2)$$

where I_{total} represents the total number of documented rockfall impacts and a_{mean} the mean age of trees in the cell.

Modeling rockfall trajectories with Rockyfor3D (v5.0)

Rockfall trajectories were simulated with Rockyfor3D (Dorren, 2012), a probabilistic process-based rockfall model that simulates trajectories of single, individually falling rocks in three dimensions. On the basis of a digital elevation model (DEM, 2 m \times 2 m resolution in the present case), single trajectories are simulated by calculating sequences of classical parabolic free fall, rebounds on the slope surface and impacts against trees. Release areas were adapted from existing expert opinions (BEG, Bureau d'Etudes Géologiques SA, 2006), to which we added steep rockfall zones with slopes contained between 60° and 90°. Release areas were used as model input in the form of (rasterized) polygon shapes without further adjustment (such as e.g. weighting). Further input parameters included slope surface roughness, soil energy dissipation capacity, forest density and mean DBH; this data was gathered by field mapping and orthophoto interpretation.

The main purposes of the simulation were to (i) realistically reproduce trajectories of falling rocks that caused damage in trees in the past, (ii) quantify natural deposition on the slope between analysis cells for which tree-ring data were obtained

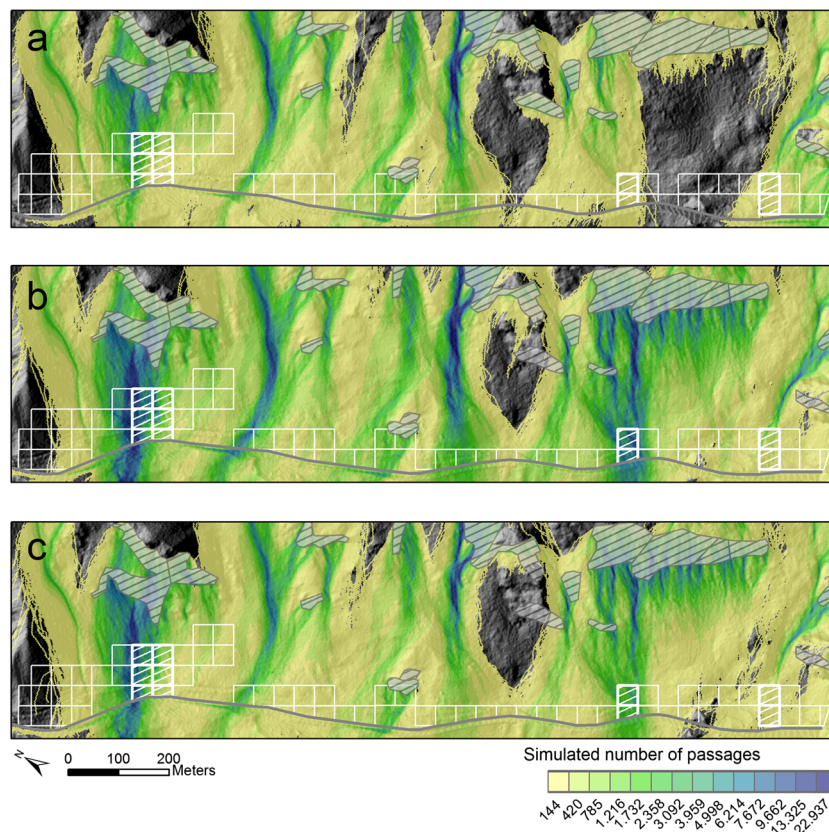


Figure 6. Simulated number of rock passages using different sets of input parameters. Note the remarkable difference in results between simulations using (a) the overall mean block diameter mapped in the field and (b) mean block diameters mapped for homogeneous sections (see Figure 5) in the south-eastern part of the slope; (c) 'best' simulated passages after model calibration (Calibration 7) using tree impact data collected in the hatched cells. This figure is available in colour online at wileyonlinelibrary.com/journal/espl

and the level of the road, and to (iii) apply the resulting reduction factor to the tree-ring record obtained for each cell.

After a first set of test simulations using the overall mean block size for the study area (i.e. 0.62 m for all three axis, see Figure 6a), trajectories could not be adequately reproduced, especially in areas with important roughness (scree slopes). We therefore defined design block sizes based on the analysis of recent deposits in the field (Figure 5) using mean volumes of blocks identified in homogeneous zones. Five design blocks with an edge length ratio of 3:2:1 were used as model input for subsequent simulation runs from the corresponding release areas (Table II) and with the aim of calibrating the model. To obtain sufficiently stable outputs, each simulation run was performed with 100 simulated blocks from each of the 21 164 source cells, resulting in a total number of 2 116 400 simulated trajectories.

The model was iteratively calibrated by performing 10 exploratory simulation runs aiming at an optimized reproduction of downslope variation of real rockfall frequencies. After each run, we compared the decline in the number of simulated passages in selected trees to the decline of real frequency as observed in the trees and tree-ring data. To visualize the decline in the observational dataset, we clustered the analysis cells into four larger groups (10 cells in total, for location see Figure 6) where cells were arranged above each other and showed a reliable reduction of real rockfall frequencies in the downslope direction. We then calculated and compared ratios of simulated passages with real frequencies. Absolute values of ratio differences were then analyzed for individual simulation runs and minimized by iterative, yet moderate changes in model input parameters. We namely adapted the block form, random variation of block sizes, tree diameters and surface roughness. Only the 'best' simulation where the sum of absolute ratio differences between model and field was smallest was kept for further analysis (Calibration 7 in Table III). It uses an ellipsoidal block form, random variation of block size

of $\pm 5\%$, additional initial fall height of 0.5 m and includes the forest as an obstacle for falling rocks.

Combining real frequencies and simulated trajectories

As analysis cells were defined within a fixed grid and not adapted to topography, falling rocks will not necessarily enter the cell located directly underneath or the road section located exactly below the investigated cell. In consequence, analysis cells were grouped into 16 zones with homogeneous rockfall activity so as to increase reliability of the results from the analysis of impacts in trees. Grouping was performed according to simulated trajectories and based on the similarity of reconstructed rockfall frequencies. To calculate rockfall frequencies for homogeneous zones, we (i) calculated mean values of cells aligned in a column and corresponding to one homogeneous zone (so as to count the passages only once), (ii) summed up the mean values from adjacent columns (in case that the road section was longer than the width of one cell) and (iii) multiplied the frequency by a reduction factor representing the reduction in simulated rock passages. The reduction factor was obtained by statistical analysis of the Rockyfor3D output raster 'number of passages'. The mean number of simulated passages at each observation screen – a linear feature representing the upslope border of the road to the analysis cells – was divided by the mean number of rock passages in those cells of the homogeneous zone located earlier, as illustrated in Figure 7. The values in the cells represent rockfall frequency

Table II. Design blocks for simulation of rockfall trajectories

| Design block | Column | Volume (m ³) | Axis lengths (m) | | |
|--------------|--------|--------------------------|------------------|------|------|
| | | | A | B | C |
| 1 | 1–4 | 0.01 | 0.36 | 0.24 | 0.12 |
| 2 | 5–8 | 0.75 | 1.5 | 1 | 0.5 |
| 3 | 9–28 | 0.16 | 0.9 | 0.6 | 0.3 |
| 4 | 29–35 | 0.75 | 1.5 | 1 | 0.5 |
| 5 | 36–41 | 0.04 | 0.57 | 0.38 | 0.19 |

Table III. Change in model input parameters during the calibration process

| Calibration | 1 | 2 | 3 | 4 | 5 | 6 | 7 | 8 | 9 | 10 |
|---|----------------------------|----------------------------|---------------------------|----------|------------|-----------|-----------|-----------|----------------------------|---------------------------|
| Variation in block volume ($\pm\%$) | ± 10 | ± 50 | ± 5 | ± 5 | ± 5 | ± 5 | ± 5 | ± 5 | ± 50 | ± 5 |
| Block form | r | r | r | e | e | e | e | e | r | e |
| Surface roughness 'rg10' ($\pm m$) ^a | — | — | — | — | 0.1 | 0.1 | 0.1 | 0.1 | 0.1 | 0.1 |
| Soil type adaption ^b | — | — | — | — | — | a1 | a2 | a2 | a2 | a2 |
| Tree diameter adaption ^b | — | — | — | — | — | — | — | a1 | a1 | a2 |
| Total absolute ratio difference ^c | 1.41 | 1.41 | 1.40 | 1.32 | 1.24 | 1.22 | 1.18 | 1.35 | 1.24 | 1.29 |

Note: Parameters shown in bold typeface indicate an adaption compared to the previous simulation run; r stands for rectangular block form, e for ellipsoidal block form. For soil type and tree diameter adaption is given as 'adaption version' (a1, a2) as soon as parameters were modified (\pm one soil type class maximum) or when parameters in the input tree file were adapted moderately based on user experience.

^aVariation from mapped parameters.

^bAdaption version compared to initial parameters.

^cFor explanation see text

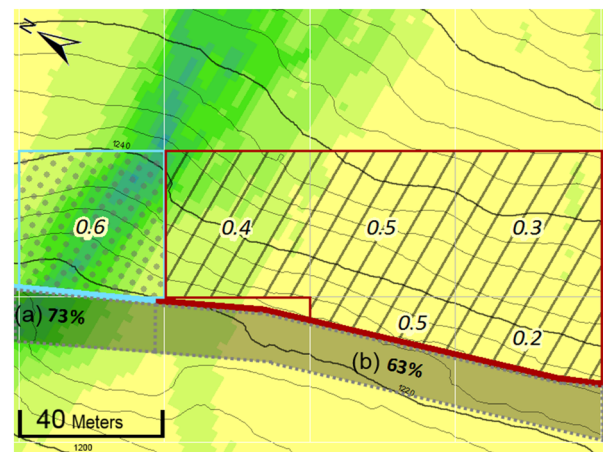


Figure 7. Example for extrapolation of rockfall frequencies observed in cells above the road to the level of the road. This figure is available in colour online at wileyonlinelibrary.com/journal/esp

and the values below the cells represent the reduction in rockfall passages (in %). For the homogeneous section (a) and (b), the frequency of rockfall was calculated as follows:

Frequency of rockfall at road section(a) = $0.6 \times 73\%$

Frequency of rockfall at road section(b) = $(0.4 + \frac{1}{2} (0.5 + 0.5) + \frac{1}{2} (0.3 + 0.2)) \times 63\%$

Results

Tree age and rockfall impacts

Analysis included 1260 trees in 64 cells ($40 \text{ m} \times 40 \text{ m}$). The number of trees analyzed per cell as well as tree age are provided in Figures 8a and b. Tree ages range from 14 to 176 yr with a mean age of 57 (standard deviation 25) yr. The oldest trees are located in the south-eastern part of the slope, whereas trees are generally younger in the central part of the study reach.

We document a total of 488 impact scars in the trees. A majority of trees did not show signs of impacts (68%) and the most heavily impacted trees showed up to four scars. At the level of the cells, the number of recorded impacts varied between zero and 35, with an average of 7.6 (standard deviation 7.8) impacts per cell.

Extrapolated rockfall frequencies using simulation results

The data gathered with tree and tree-ring analysis was then used to calibrate the rockfall model. The simulated rockfall passages – as illustrated in Figure 9 – are in good agreement with the reconstructed rockfall activity as observed on and in trees. Model and observation also agree on the zones where rockfall activity is increased and where forest is less affected by falling rocks and boulders. The model also illustrates that an important proportion of falling rocks (up to 73%) is deposited in some segments of the study area well before they reach the road. In other zones, preferential paths can be detected where blocks might more easily reach the road. The good agreement between real rockfall frequencies and simulated passages therefore clearly allows extrapolation of the real frequencies in the following step.

Figure 10 represents the rockfall passages at the level of the road and is a combination of observed, tree-ring based data

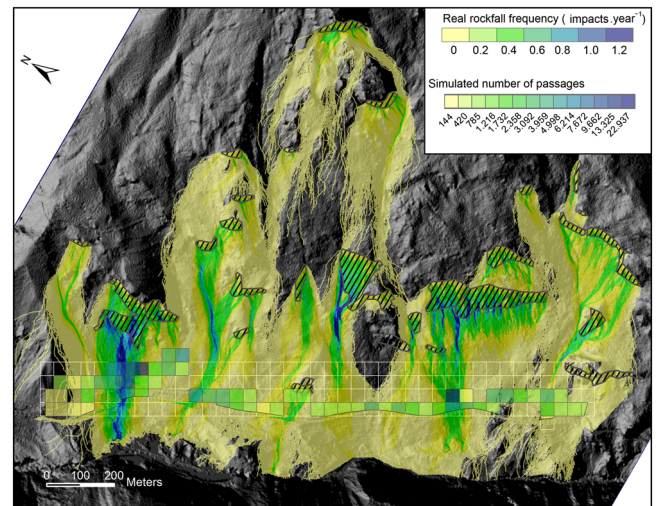


Figure 9. Simulated number of passages (Rockyfor3D) and real rockfall frequency as observed on trees given as passages per year; values represent the upper class limits. This figure is available in colour online at wileyonlinelibrary.com/journal/esp

and simulation output. The latter was used in this context to determine a reduction factor based on the amount of rocks being deposited between the lowermost cell and the level of the road. The reduction of passages for zones of homogeneous rockfall activity is presented in Figure 10b. As a result we obtain a mean of nine rocks per year reaching or passing the 1631-m long road section. The rockfall frequency at the level of the road is presented with normalized values and indicates the number of rock passages per meter road length for each of the homogeneous units. Results point to largely differing rockfall activity between the different sections and point to a series of hotspots of rockfall activity and to zones with less frequent rockfalls. Frequencies in the homogeneous zones range from 0.0006 to 0.0177 passages per year and running meter and result in a mean number of passages per year and running meter of 0.0065.

Discussion

A full assessment of rockfall hazards requires the evaluation of (i) the temporal probability (in terms of frequency normalized to the surface unit) and spatial susceptibility of rockfalls, (ii) 3D

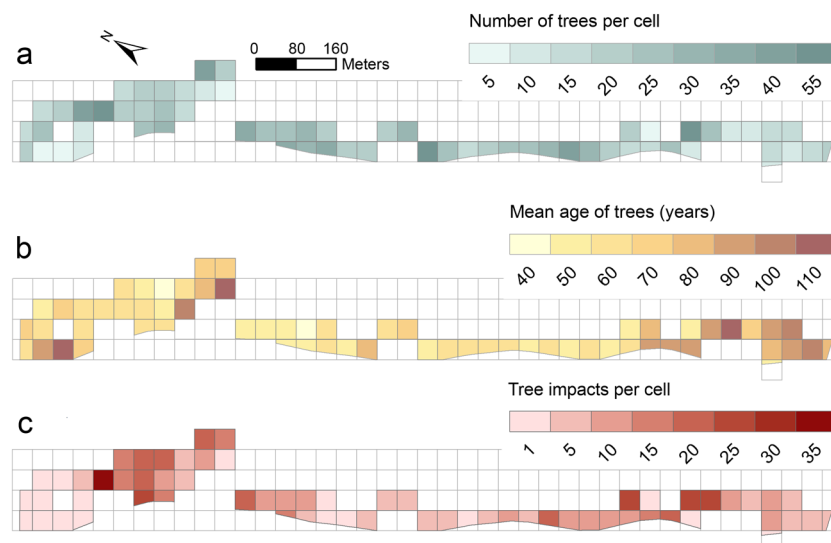


Figure 8. (a) Number of investigated trees per cell; (b) mean tree age per cell; (c) number of tree impacts per cell; values represent the upper class limits. This figure is available in colour online at wileyonlinelibrary.com/journal/esp

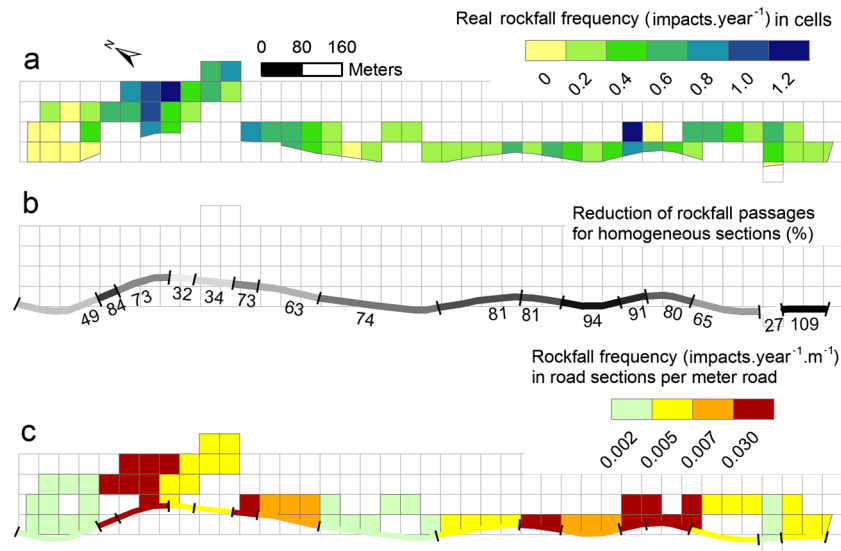


Figure 10. (a) Rockfall frequency derived from tree data in analysis cells; (b) reduction of passages according to simulated trajectories (Rockyfor3D) for homogeneous zones; (c) extrapolated rockfall frequencies at the level of the road per running meter for homogeneous zones; values represent the upper class limits. This figure is available in colour online at wileyonlinelibrary.com/journal/espl

trajectories, (iii) maximum runout distances of rocks and boulders, and (iv) rockfall intensity (in terms of energy) at each location along the paths of falling rocks (Corominas and Moya, 2008; Volkwein *et al.*, 2011). The combination of 3D, process-based rockfall simulation models and impact data on trees contributes to the requirements of comprehensive hazard assessments and provides a series of advantages which complement traditional management practices.

Advantages of using combined modeling and tree data approaches

One major limitation of pure modeling approaches in the past has been the lack of information on the temporal probability and thus the representation of model output in terms of real frequencies. This shortcoming can be overcome by merging model and field data and by translating simulated rock passages into rockfall frequencies in terms of return periods (Corona *et al.*, 2013).

Insufficient historical data represent yet another critical point and often hampers the calibration and validation of simulation results with observations. The impact of lacking archival data on physically based process models, such as Rockyfor3D, is generally acceptable as they are typically based on a large number of field tests. Nevertheless, results from this study demonstrate that the definition of representative block sizes and smaller modifications of input parameters – mapped in the field or on orthophotos – can improve the reproduction of trajectories quite substantially.

The coupling of modeling with tree-ring approaches also helps to overcome one of the key issues in dendrogeomorphology, namely the need of having trees growing at the location of interest. With the proposed methodology, rockfall impacts on trees can be analyzed at almost any location on the slope that is suitable for dendrogeomorphic analysis. The resulting rock passages observed in the tree-ring record can then be interpolated to the location of interest by using calibrated simulation results. Nevertheless, and with the idea of keeping uncertainty to a strict minimum, an investigation of trees in direct proximity to the location of interest is still preferable.

The combined analysis of mature conifers with classic dendrogeomorphic techniques and young conifers and broad-leaves with a scar-count approach allows the inclusion of a large set of trees to be analyzed with reasonable temporal efforts. In a similar way, the calculation of frequencies at the level of cells allows the inclusion of trees with and without impacts in a meaningful way. Unaffected trees have been excluded in the past but are expected to yield valuable additional insight into real rockfall activity, in particular on slopes with limited rockfall activity. In addition, relative rockfall frequencies become comparable between individual zones which in turn enables a spatial differentiation and prioritization of protection measures at the site. The positioning and design is furthermore facilitated by the large number of trees for which bounce heights are available.

Reliability of 'real rockfall frequency' from tree-impact data

A realistic determination of rockfall frequencies (i.e. how often a rock with a certain dimension will fall from a source area or affect a certain location) is a difficult task in general and a major source of uncertainty in most hazard assessment procedures. The real rockfall frequencies of this study have been based on observations on trees; results show a mean number of nine rocks per year that reached or passed the 1631-m long road section. This number is by far higher than historical records for several reasons. One possible reason is the underreporting of smaller events by road workers and local administration. Another reason for possible discrepancies is related to the tree-ring approach where the 'real frequency' value represents a statistical long-term number of rocks per time unit affecting the road. Noteworthy, the long-term mean may differ drastically from event frequency where several blocks are involved in one rockfall. Several rocks (or rock fragments) have likely been involved in some of the events, as reported for instance for the 2006 rockfall, which can consequently result in a lower event frequency and longer return periods for events noted in written sources as compared to reconstructed frequencies. A consideration of the mean number of rocks per event (including clasts) would be necessary for an approximation of the frequency of

individual events (rather than the frequency of individual rockfall impacts). However, rockfalls consisting of several rocks will also affect a larger portion of the road by lateral spread which in turn might compensate for the hypothetical overestimation in activity.

Trappmann and Stoffel (2013) found differences in rockfall frequencies depending on the tree species investigated and the approach used. They note that scar count approaches might lead to overestimations of past rockfall activity in trees with thin bark structures as these are likely to be more sensitive to damage (with the result that one rock might inflict multiple scars in one tree). At the same time, the very effective and rather rapid blurring of scars in conifers might lead to an underestimation of rockfall activity at the same site as well. Based on these findings, we excluded scars showing similar appearance and close proximity as they were interpreted in the field as multiple scars from the same rock. The application of classical dendrogeomorphic techniques would have allowed for a more precise dating (yearly, up to seasonal) of rockfall scars in this case and would thus have facilitated the detection of multiple scars. Whereas detailed dendrogeomorphic procedures could clearly have improved the level of confidence with respect to the estimation of event frequencies, financial and temporal efforts usually limit the practical application of yearly resolved analyses of a sufficiently high number of trees on larger surfaces.

The absence of trees on certain slope sectors following high-magnitude rockfalls could also impede a meaningful investigation of process activity in some cases. At our study site, evidence of such large events could be observed but fallen trees had already been removed by forest managers. However, scars could still be found in the remaining surviving trees in close proximity and most likely as a result of rock fragment dispersal. The application of the approach suggested in this paper certainly needs careful adaptation to each study site and calls for the validation of the approaches described on sites with well documented rockfall activity in space and time (which are, unfortunately, rare).

Based on the authors' field experience, eyewitness reports, archival records and geological expert opinions, the spatial patterns of rockfall frequencies are in good agreement with observations and existing assessments at the study site.

Model calibration based on tree impact data

The main aim of rockfall simulations within this study was to obtain a measure for the decline in rockfall activity (i.e. stopping rocks) in the downslope direction, in order to quantify the amount of natural deposition between the investigated cells and the level of the road. Model calibration therefore aimed at a good agreement between simulated passages and real rockfall frequencies in the downslope direction, and did not seek to fully represent differences in rockfall occurrence perpendicular to the slope (representing lateral difference in productivity of the release zones). The agreement between the modeled and observed lateral spread across the slope resulted mainly from the channelizing effects of topography as well as from the detailed data of release areas available from geological expert opinions (BEG, Bureau d'Etudes Géologiques SA, 2006).

The model was calibrated through an iterative adoption of input parameters in the model runs rather than using a predefined variation of the parameters for the whole study site. Input parameters were adopted within the boundaries of realistic assumptions for specific zones at the study site, thereby allowing a fixation of parameters for zones where a good agreement between field and model data was achieved. The sum of absolute ratio differences served as a measure for the quality of the simulation (Table III). It is apparent that different sets of parameters can lead to

simulation results with comparable quality (e.g. Calibrations 5 and 9), so that the procedure used in this paper does not necessarily allow for an optimization of all parameters but it clearly increases the confidence in the predicted reduction of rock passages in the downslope direction.

Conclusions

The combination of 3D, physically-based modeling approaches with tree-ring data on rockfall impacts has been used to quantify the occurrence of rockfalls along a road in the Swiss Alps. The approach complements traditional hazard management by including – for the first time – extensive frequencies of rockfalls derived from tree-impact data. This allows determination of real rockfall frequencies (in terms of return intervals) and a quality assessment of the model, whereas the modeling approach enables evaluation of the statistical robustness of the dendrogeomorphic approach. Results of the field and model-based approaches are in good agreement and support each other. The procedure presented in this contribution can be used to establish hazard and risk maps based on real frequencies of past rockfalls and allows for a prioritization and dimensioning of constructive measures.

In consideration of its significant advantages, namely as far as the quantification of past rockfall frequencies are concerned, we recommend that tree-ring series be included whenever possible in future management strategies on rockfall slopes, as a target-oriented inclusion of tree-impact data can enhance hazard and risk assessments considerably with limited additional efforts, especially when it comes to the calibration of rockfall models and the transformation of rockfall susceptibilities into rockfall hazards.

Acknowledgements—The authors acknowledge the Forest and Landscape Department at the Canton of Valais and the Community of Evolène for financial support. Elisa Salaorni helped with the analysis of tree-ring samples.

References

- Abbruzzese JM, Sauthier C, Labiouse V. 2009. Considerations on Swiss methodologies for rock fall hazard mapping based on trajectory modelling. *Natural Hazards and Earth System Science* **9**: 1095–1109. DOI: 10.5194/nhess-9-1095-2009
- Agliardi F, Crosta GB. 2003. High resolution three-dimensional numerical modelling of rockfalls. *International Journal of Rock Mechanics and Mining Sciences* **40**: 455–471. DOI: 10.1016/S1365-1609(03)00021-2
- Arbellay E, Stoffel M, Bollschweiler M. 2010. Wood anatomical analysis of *Alnus incana* and *Betula pendula* injured by a debris-flow event. *Tree Physiology* **30**: 1290–1298. DOI: 10.1093/treephys/tpq065
- Arbellay E, Corona C, Stoffel M, Fonti P, Decaulne A. 2012a. Defining an adequate sample of earlywood vessels for retrospective injury detection in diffuse-porous species. *PLoS One* **7**: e38824. DOI: 10.1371/journal.pone.0038824
- Arbellay E, Fonti P, Stoffel M. 2012b. Duration and extension of anatomical changes in wood structure after cambial injury. *Journal of Experimental Botany* **63**: 3271–3277. DOI: 10.1093/jxb/ers050
- Arbellay E, Stoffel M, Decaulne A. 2013. Dating of snow avalanches by means of wound-induced vessel anomalies in sub-arctic *Betula pubescens*. *Boreas* **42**: 568–574. DOI: 10.1111/j.1502-3885.2012.00302.x
- Ballesteros JA, Stoffel M, Bollschweiler M, Bodoque JM, Diez-Herrero A. 2010. Flash-flood impacts cause changes in wood anatomy of *Alnus glutinosa*, *Fraxinus angustifolia* and *Quercus pyrenaica*. *Tree Physiology* **30**: 773–781. DOI: 10.1093/treephys/tpq031
- BEG, Bureau d'Etudes Géologiques SA. 2006. RC 54 Sion-Arolla Secteur 'Les Clièves'–'La Villette' – Zones de danger «chute de pierres et éboulement» Mesures de protection, Technical report. BEG: Aproz.

- Berger F, Dorren LKA. 2006. Objective comparison of rockfall models using real size experimental data. In *Disaster Mitigation of Debris Flows, Slope Failures and Landslides*, Marui H et al. (eds). Universal Academy Press Inc.: Tokyo; 245–252.
- Berger F, Quétel C, Dorren LKA. 2002. Forest: a natural protection mean against rockfall, but with which efficiency? The objectives and methodology of the ROCKFOR project. *Interpraevent* **2**: 815–826.
- Bosch O, Gutiérrez E. 1999. La sucesión en los bosques de pinus uncinata del pirineo. De los anillos de crecimiento a la historia del bosque. *Ecología* **13**: 133–171.
- Bräker OU. 2002. Measuring and data processing in tree-ring research — a methodological introduction. *Dendrochronologia* **20**: 203–216.
- Corominas J, Moya J. 2008. A review of assessing landslide frequency for hazard zoning purposes. *Engineering Geology* **102**: 193–213. DOI: 10.1016/j.enggeo.2008.03.018
- Corominas J, Copons R, Moya J, Vilaplana JM, Altimir J, Amigó J. 2005. Quantitative assessment of the residual risk in a rockfall protected area. *Landslides* **2**: 343–357. DOI: 10.1007/s10346-005-0022-z
- Corona C, Trappmann D, Stoffel M. 2013. Parameterization of rockfall source areas and magnitudes with ecological recorders: when disturbances in trees serve the calibration and validation of simulation runs. *Geomorphology*. DOI: 10.1016/j.geomorph.2013.02.001
- Crosta GB, Agliardi F. 2003. A methodology for physically based rockfall hazard assessment. *Natural Hazards and Earth System Science* **3**: 407–422. DOI: 10.5194/nhess-3-407-2003
- Dorren LKA. 2012. *Rockyfor3D (v 5.0) Revealed – Transparent Description of the Complete 3D Rockfall Model*, ecorisQ paper. Association ecorisQ: Saint Hilaire du Touvet. <http://www.ecorisq.org> [6 December 2012].
- Dorren LKA, Berger F. 2006. Balancing tradition and technology to sustain rockfall-protection forests in the Alps. *Forest Snow and Landscape Research* **80**: 87–98.
- Dorren LKA, Domaas U, Kronholm K, Labiouse V. 2011. Methods for predicting rockfall trajectories and run-out zones. In *Rockfall Engineering*, Lambert S, Nicot F (eds). ISTE Ltd/John Wiley & Sons: New York; 143–173.
- Dussauge-Peisser C, Helmstetter A, Grasso J-R, Hantz D, Desvarreux P, Jeannin M, Giraud A. 2002. Probabilistic approach to rock fall hazard assessment: potential of historical data analysis. *Natural Hazards and Earth System Science* **2**: 15–26.
- Guzzetti F, Reichenbach P, Ghigi S. 2004. Rockfall hazard and risk assessment along a transportation corridor in the Nera Valley, central Italy. *Environmental Management* **34**: 191–208. DOI: 10.1007/s00267-003-0021-6
- Jaboyedoff M, Dudt JP, Labiouse V. 2005. An attempt to refine rockfall hazard zoning based on the kinetic energy, frequency and fragmentation degree. *Natural Hazards and Earth System Science* **5**: 621–632.
- Lateltin O, Haemmig C, Raetzo H, Bonnard C. 2005. Landslide risk management in Switzerland. *Landslides* **2**: 313–320. DOI: 10.1007/s10346-005-0018-8
- Matsuoka N. 2008. Frost weathering and rockwall erosion in the southeastern Swiss Alps: long-term (1994–2006) observations. *Geomorphology* **99**: 353–368. DOI: 10.1016/j.geomorph.2007.11.013
- Michoud C, Derron M-H, Horton P, Jaboyedoff M, Baillifard F-J, Loye A, Nicolet P, Pedrazzini A, Queyrel A. 2012. Rockfall hazard and risk assessments along roads at a regional scale: example in Swiss Alps. *Natural Hazards and Earth System Science* **12**: 615–629. DOI: 10.5194/nhess-12-615-2012
- Moya J, Corominas J, Arcas JP. 2010a. Assessment of the rockfall frequency for hazard analysis at Solà d'Andorra (eastern Pyrenees). In *Tree Rings and Natural Hazards*, Stoffel M, Bollschweiler M, Butler DR, Luckman BH (eds). Springer: Berlin; 161–175.
- Moya J, Corominas J, Pérez Arcas J, Baeza C. 2010b. Tree-ring based assessment of rockfall frequency on talus slopes at Solà d'Andorra, eastern Pyrenees. *Geomorphology* **118**: 393–408. DOI: 10.1016/j.geomorph.2010.02.007
- Raetzo H, Lateltin O, Bollinger D, Tripet J. 2002. Hazard assessment in Switzerland – Codes of Practice for mass movements. *Bulletin of Engineering Geology and the Environment* **61**: 263–268. DOI: 10.1007/s10064-002-0163-4
- Rozas V. 2003. Tree age estimates in *Fagus sylvatica* and *Quercus robur*: testing previous and improved methods. *Plant Ecology* **167**: 193–212.
- Šilhán K, Brázdil R, Pánek T, Dobrovolný P, Kašičková L, Tolasz R, Turský O, Václavek M. 2011. Evaluation of meteorological controls of reconstructed rockfall activity in the Czech Flysch Carpathians. *Earth Surface Processes and Landforms* **36**: 1898–1909. DOI: 10.1002/esp.2211
- Šilhán K, Pánek T, Hradecký J. 2012. Tree-ring analysis in the reconstruction of slope instabilities associated with earthquakes and precipitation (the Crimean Mountains, Ukraine). *Geomorphology* **173–174**: 174–184. DOI: 10.1016/j.geomorph.2012.06.010
- Stoffel M, Bollschweiler M. 2008. Tree-ring analysis in natural hazards research – an overview. *Natural Hazards and Earth System Science* **8**: 187–202. DOI: 10.5194/nhess-8-187-2008
- Stoffel M, Wehrli A, Kühne R, Dorren LKA, Perret S, Kienholz H. 2006. Assessing the protective effect of mountain forests against rockfall using a 3D simulation model. *Forest Ecology and Management* **225**: 113–122. DOI: 10.1016/j.foreco.2005.12.030
- Stoffel M, Bollschweiler M, Butler DR, Luckman BH. 2010. *Tree Rings and Natural Hazards*. Springer: Berlin.
- Trappmann D, Stoffel M. 2013. Counting scars on tree stems to assess rockfall hazards: a low effort approach, but how reliable? *Geomorphology* **180–181**: 180–186. DOI: 10.1016/j.geomorph.2012.10.009
- Trappmann D, Corona C, Stoffel M. 2013. Rolling stones and tree rings: a state of research on dendrogeomorphic reconstructions of rockfall. *Progress in Physical Geography* **37**: 701–716. DOI: 10.1177/0309133313506451
- Varnes DJ. 1978. Slope movement types and processes. In *Landslides: Analysis and Control*, Schuster RL, Krizek RJ (eds). National Academy of Science: Washington, DC; 11–33.
- Volkwein A, Schellenberg K, Labiouse V, Agliardi F, Berger F, Bourrier F, Dorren LKA, Gerber W, Jaboyedoff M. 2011. Rockfall characterisation and structural protection – a review. *Natural Hazards and Earth System Science* **11**: 2617–2651. DOI: 10.5194/nhess-11-2617-2011